



# High-order mutants reveal an essential requirement for peroxidases but not laccases in Casparian strip lignification

Nelson Rojas-Murcia<sup>a,1</sup>, Kian Hématy<sup>a</sup>, Yuree Lee<sup>a,b,2</sup>, Aurélia Emonet<sup>a</sup>, Robertas Ursache<sup>a</sup>, Satoshi Fujita<sup>a,3</sup>, Damien De Bellis<sup>a,4</sup>, and Niko Geldner<sup>a,5</sup>

<sup>a</sup>Department of Plant Molecular Biology, Biophore, University of Lausanne, CH-1015 Lausanne, Switzerland; and <sup>b</sup>Plant Genomics and Breeding Institute, Seoul National University, 08826 Seoul, Republic of Korea

Edited by Natasha V. Raikhel, Center for Plant Cell Biology, Riverside, CA, and approved September 30, 2020 (received for review June 19, 2020)

Lignin has enabled plants to colonize land, grow tall, transport water within their bodies, and protect themselves against various stresses. Consequently, this polyphenolic polymer, impregnating cellulosic plant cell walls, is the second most abundant polymer on Earth. Yet, despite its great physiological, ecological, and economical importance, our knowledge of lignin biosynthesis *in vivo*, especially the polymerization steps within the cell wall, remains vague—specifically, the respective roles of the two polymerizing enzymes classes, laccases and peroxidases. One reason for this lies in the very high numbers of laccases and peroxidases encoded by 17 and 73 homologous genes, respectively, in *Arabidopsis*. Here, we have focused on a specific lignin structure, the ring-like Casparian strips (CSs) within the root endodermis. By reducing candidate numbers using cellular resolution expression and localization data and by boosting stacking of mutants using CRISPR-Cas9, we mutated the majority of laccases in *Arabidopsis* in a nonuple mutant—essentially abolishing laccases with detectable endodermal expression. Yet, we were unable to detect even slight defects in CS formation. By contrast, we were able to induce a complete absence of CS formation in a quintuple peroxidase mutant. Our findings are in stark contrast to the strong requirement of xylem vessels for laccase action and indicate that lignin in different cell types can be polymerized in very distinct ways. We speculate that cells lignify differently depending on whether lignin is localized or ubiquitous and whether cells stay alive during and after lignification, as well as the composition of the cell wall.

lignin | endodermis | roots | cell wall | Casparian strip

Casparian strips (CSs) are highly conserved structures that are a defining feature of the root endodermis in higher plants. That CSs are of a lignin-like nature had been proposed repeatedly since their discovery in the 19th century and was firmly established by modern histological and genetic analyses in the model plant *Arabidopsis* (1, 2). CSs are strictly localized cell wall impregnations, forming as longitudinal, centrally located belts between endodermal cells. Their highly coordinated and simultaneous appearance in endodermal neighbors leads to the fusion of these belts into a supracellular structure that takes the appearance of a delicate network, due to the very thin primary cell walls of young endodermal cell (100 to 200 nm in width). Using lignin stains, this fine network can be easily overlooked, next to the much more pronounced lignification occurring at the same time in the thick secondary cell walls of protoxylem vessels, only two cell layers below within the vasculature. The CSs therefore represent only a minor fraction of the overall lignin content of a root and are always found in close association to the xylem, making it very difficult to use the classical chemical methods of lignin analysis that are central to the field. Yet, CSs are very attractive for cell biological and genetic analyses for a number of reasons. The endodermis can be observed in very young, 5-d-old seedlings, and it is a relatively peripheral, large cell type that is more easily observed than cell types in the vasculature. Moreover,

its highly predictable and restricted lignification allows for meaningful spatial correlations between protein localization and lignin deposition. Finally, the endodermis stays alive during and after the entire process of lignification (3). Using the endodermis as a model, we were able to establish a strong requirement for reactive oxygen species (ROS) production in CS lignification. Knockouts of a single NADPH oxidase, respiratory burst oxidase homolog F (RBOHF), led to a near absence of lignification in the endodermis, as did inhibitor treatments interfering with ROS production or accumulation (2). Intriguingly, RBOHF specifically accumulates at the site of CS formation, which is initiated by the accumulation of CASPARIAN STRIP MEMBRANE DOMAIN PROTEINS (CASPs), small transmembrane scaffold proteins that are thought to recruit RBOHF and other proteins to their site of action. Another class of proteins that appear to be localized by

## Significance

Lignin is a defining polymer of vascular plants and of great physiological, ecological, and economical importance. Yet, its polymerization in the cell wall is still not understood. Lignin polymerizing enzymes, laccases and peroxidases, exist in vast numbers in plant genomes. By focusing on a specific lignin structure, the ring-like Casparian strips (CSs), we reduced candidate numbers and abolished essentially all laccases with detectable endodermal expression. Yet, not even slight defects in CS formation were detected. By contrast, a quintuple peroxidase mutant displayed a complete absence of CS. Our findings suggest that cells lignify differently depending on whether lignin is localized or ubiquitous and whether cells stay alive during and after lignification, as well as the composition of the cell wall.

Author contributions: N.R.-M., K.H., Y.L., S.F., and N.G. designed research; N.R.-M., K.H., Y.L., A.E., R.U., S.F., and D.D.B. performed research; N.R.-M., K.H., Y.L., R.U., and S.F. contributed new reagents/analytic tools; N.R.-M., K.H., R.U., S.F., D.D.B., and N.G. analyzed data; and N.R.-M. and N.G. wrote the paper.

The authors declare no competing interest.

This article is a PNAS Direct Submission.

This open access article is distributed under [Creative Commons Attribution-NonCommercial-NoDerivatives License 4.0 \(CC BY-NC-ND\)](https://creativecommons.org/licenses/by-nc-nd/4.0/).

<sup>1</sup>Present address: Umeå Plant Science Centre, Department of Plant Physiology, Umeå University, SE-901 87 Umeå, Sweden.

<sup>2</sup>Present address: School of Biological Sciences, Seoul National University, 08826 Seoul, Republic of Korea.

<sup>3</sup>Present address: National Institute of Genetics, Department of Gene Function and Phenomics, Mishima, 411-8540 Shizuoka, Japan.

<sup>4</sup>Present address: Electron Microscopy Facility, University of Lausanne, 1015 Lausanne, Switzerland.

<sup>5</sup>To whom correspondence may be addressed. Email: Niko.Geldner@unil.ch.

This article contains supporting information online at <https://www.pnas.org/lookup/suppl/doi:10.1073/pnas.2012728117/-DCSupplemental>.

First published November 2, 2020.

CASPs is type III peroxidases (PER). Among those, PER64 showed an especially strict colocalization with CASP1. Indeed, transfer DNA (T-DNA) insertion- and artificial microRNA (amiRNA)-driven knockout/knockdown of multiple endodermis-expressed and CS-localized peroxidases led to a delay of barrier formation (2), although the severity and nature of lignin defects were not assessed at that time. These findings led to a model whereby CASPs are acting to bring together NADPH oxidase and peroxidase, effectively allowing channel-localized ROS production toward peroxidases, thus ensuring localized and efficient lignification (2). Clearly, localized presence of RBOHF and peroxidases is sufficient for localizing lignification since complementation of monolignol-deficient plants with large amounts of external monolignols did not affect localization of CS formation (1). More recently, we showed that a dedicated receptor pathway in the endodermis can detect defects in the CS diffusion barrier and initiate compensatory, ectopic lignification in cell corners, both by enhancing ROS production from RBOHF and RBOHD and inducing expression of genes, including additional peroxidases and laccases (*LAC*) (4–6). Our findings demonstrating a strong requirement for ROS production and a partial genetic requirement for peroxidases was in contrast with the finding that LACCASES (*LACs*) are necessary for lignification of xylem vessels, fibers, and other cell types. *LACs* are glycosylated, multicopper enzymes that catalyze the oxidation of various phenolic substrates using  $O_2$  as final electron acceptor, not requiring  $H_2O_2$  (7, 8). *LAC15* was found to express in seed coats, its loss-of-function mutant displaying a 30% reduction of lignin in seeds (9, 10). *LAC4*, also called *IRREGULAR XYLEM 12* (11), and *LAC17* are expressed in vessels and xylary fibers in the stem (12). *LAC4* localizes to secondary cell wall domains of proto- and metaxylem vessels, as well as vessels, xylary, and interfascicular fibers of inflorescence stems (12–15). Mutant lines of *lac4* and *lac4 lac17* have collapsed xylem vessels and reduced lignin content in total stem biomass (12). The reduction in lignin content of the double mutant was further enhanced in the presence of an *lac11* mutant, which showed severe developmental defects and stopped growing after developing the two first pair of leaves (16). Finally, *LAC15* and *LAC7* are expressed in lignifying cells in the context of floral organ abscission, although it was not demonstrated whether mutations of both *LACs* affected lignin deposition in this context (17). More recently, *LAC2* was found to negatively regulate overlignification in the root vasculature upon phosphate and water deficiency. Nevertheless, the exact role of *LAC2* in such context was not determined (18).

Yet, numerous studies have also provided evidence for participation of PERs in lignification outside of the endodermis. In the *Arabidopsis* stem xylem vessels, mutations of *PERs* partially impact lignification (19, 20). It was proposed that both enzymes act sequentially in the lignin polymerization of a same cell type, although it has not been excluded that they individually lignify different cell types (8, 15, 21). Cell cultures of the gymnosperm Norway spruce release lignin polymers into the growth medium (22). Scavenging of  $H_2O_2$  prevents production of this extracellular lignin, and phenolic profiling of the culture media of scavenger-treated cell cultures revealed the accumulation of specific oligolignols (21). This led the authors to propose that  $H_2O_2$ -independent enzymes, such as laccases, mediate formation of oligolignols, while peroxidases would be required for further polymerization. However, the authors could not exclude the possibility that in their treatment to scavenge  $H_2O_2$ , a residual PERs activity was present (21). Unfortunately, participation of PER in lignification in planta has often been inferred from the use of inhibitors of PERs or  $H_2O_2$  production (2, 23), while genetic evidence could reveal only weak, partial effects on lignification, allowing for the possibility that peroxidases are only peripheral actors of lignification in planta.

In addition to PERs, data of cell type-specific gene expression have revealed that *LACs* are expressed in the endodermis (24–27). Considering the evidence on the role of *LACs* in lignification, we took advantage of the experimental setup offered by the endodermis to conduct a genetic analysis of *LACs* in order to determine whether they contribute to lignin polymerization in the CS.

In this work, we set out to determine whether one given lignin structure in a cell requires either laccases or peroxidases exclusively or whether its formation requires a combination of both enzyme classes. Using the endodermal CS as a model, we demonstrate that a number of laccases show specific expression in the endodermis and localization to the CS, yet generation of a nonuple mutant, mutating the vast majority of laccases with detectable endodermal expression, had no discernable effect on CS lignification or formation of the endodermal barrier. By contrast, generating a quintuple mutant of endodermis-enriched peroxidases led to a complete absence of CS lignification. Abrogating the compensatory lignification by the SCHENGEN pathway even led to a complete absence of any lignification in young endodermal cells.

Based on this, it is most parsimonious to conclude that, despite their strong presence, laccases are fully replaceable for lignification of CS, while peroxidases are absolutely required.

## Results

**Selection of Candidate *LACs* for Endodermal CS Formation.** A reverse genetic analysis of *LACs* involved in lignification of the CS is challenging due to the fact that there are 17 encoding *LAC* genes in *Arabidopsis* with evidence for functional redundancy between them (12, 16). Data of cell type-specific gene expression available for the *Arabidopsis* root are a powerful tool to guide such an effort (26–28). We found that a set composed of *LAC1*, -3, -5, -13, and -16 displayed enriched messenger RNA (mRNA) expression in the endodermis (*SI Appendix, Fig. S1 A and B*). *LAC8* displayed strong expression across different cell types/root zones, including the endodermis (*SI Appendix, Fig. S1 A and B*), but since it was not enriched in endodermis, we decided to use *LAC1*, -3, -5, -13, and -16 in the first step.

***LAC1*, *LAC3*, *LAC5*, and *LAC13* Promoter Reporters Corroborate Endodermal Expression.** We generated transcriptional reporters of *LAC1*, -3, -5, -13, and -16 by fusing their upstream regulatory sequences to a nuclear localization signal (nls)-GFP-GUS reporter gene. We observed expression in the endodermis for all lines except p*LAC16*, which could not be detected either as GFP or after extended GUS staining. CS formation/lignification occurs in a reproducible spatial pattern, starting between six and eight cells after onset of elongation (exit from the meristem). After rapid progression into an uninterrupted network, CSs slowly broaden, and lignin stains increase in intensity until a region of about two-thirds of the root length—in 5-d-old seedlings—at which CASP proteins start to disappear and suberin lamellae start to sever the direct contact between the CS and the plasma membrane. At this point, it can be presumed that CS lignification has ceased completely. Genes involved in CS lignification can therefore be predicted to follow this spatial pattern, an aspect that can be assessed by promoter lines but is insufficiently resolved in cell type-specific expression databases.

We found that expression in the p*LAC1* line was observed six cells after onset of elongation, starting in the stele. Only at about 16 cells, a GFP signal could additionally be observed in the endodermis (Fig. 1A and *SI Appendix, Fig. S2A*). In later root developmental stages, expression became exclusive to the endodermis extending until two-thirds of the total primary root length.

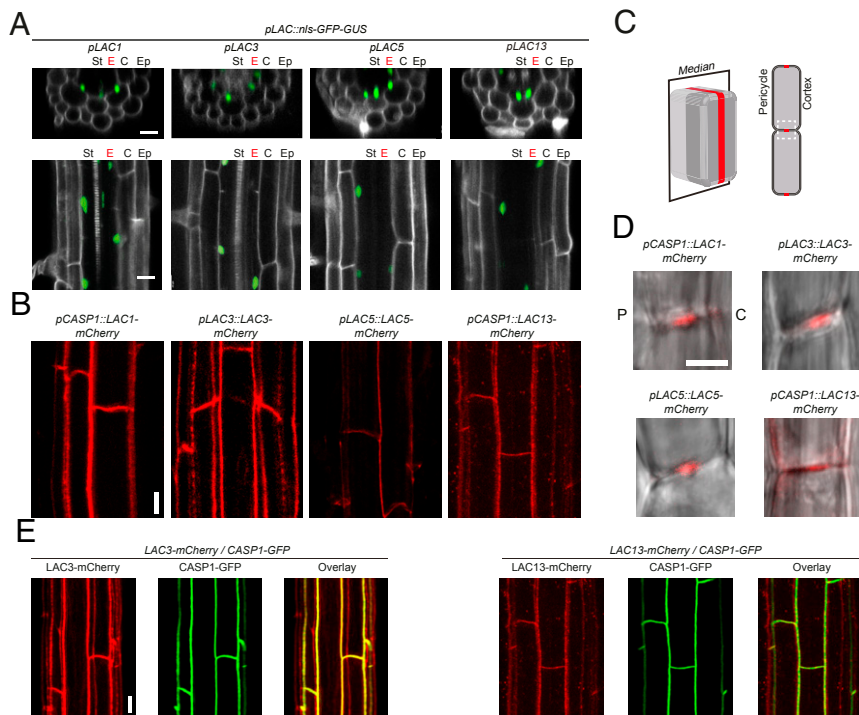


**Fig. 1.** LACs are expressed in the endodermis and targeted to the CS. (A) Overview of expression pattern of *pLAC::nls-GFP-GUS* transcriptional reporters in 5-d-old roots of *A. thaliana* for *LAC1*, *LAC3*, *LAC5*, and *LAC13*. Pictures show the overlay of GFP (green) and PI (gray). (Upper) Optical transversal sections. (Lower) Optical longitudinal sections. C, cortex; E, endodermis (in red to emphasize its position); Ep, epidermis; St, stele. (B) Surface overview (z-axis maximum projection) of C-terminal, mCherry-4G-tagged proteins of *LAC1*, *LAC3*, *LAC5*, and *LAC13* localization in the endodermis. (C) Schematic of endodermal cell, explaining optical section shown in D. Schematic adapted from ref. 40. (D) The four LACs localize to the median position of the endodermis cell wall where the CS is located. Overlay of mCherry-4G signal in red with transmitted light in gray, highlighting the cell contour. Other legends are the same as in A. C, cortex; P, pericycle. (E) C-terminal, fluorescently tagged proteins *pLAC3::LAC3-mCherry-4G* and *pCASP1::LAC13-mCherry-4G* colocalize with CASP1-GFP, which marks the membrane domain of the CS. The mCherry picture in this panel is identical to that of *LAC13-mCherry* in B. In B, D, and E, the expression of *LAC1* and *LAC13* fusion constructs was driven by the CASP1 promoter (*pCASP1*) owing to low and unstable expression observed with native promoter fragments. (Scale bars: A, 20  $\mu$ m; B and E, 10  $\mu$ m; D, 5  $\mu$ m.)

GFP expression in *pLAC3*, *pLAC5*, and *pLAC13* lines was observed exclusively in the endodermis (Fig. 1A). However, their onset of expression varied among the three promoters, taking place after circa (ca.) 6, 9, and 25 endodermal cells for *pLAC3*, *pLAC5*, and *pLAC13*, respectively. Additionally, while *pLAC3* and *pLAC13* expression was strong all along their expression domain, *pLAC5* expression became stronger in later root developmental stages (SI Appendix, Fig. S24). Expression in all three promoter lines extended until the hypocotyl.

A previous report using *GUS* transcriptional reporters showed that a *pLAC7* line drove strong expression in the root (29). We generated a *pLAC7::nls-GFP-GUS* line and found strong expression of GFP in epidermis and cortex, but not in the endodermis (SI Appendix, Fig. S2B). Taken together, the identified LAC promoter activities nicely matched the developmental zones where lignin deposition is observed in the CS (30), confirming and extending on the available public expression profile databases.

**Protein Fusions of *LAC1*, *LAC3*, *LAC5*, and *LAC13* Accumulate at the Site of CS Formation.** The strict, CASP-dependent localization of lignification within endodermal cell walls allows us to predict that enzymes involved in lignin polymerization should accumulate at CS and colocalize with CASPs. We therefore generated plants expressing C-terminal, mCherry fusion constructs, under the control of their own, or of the strong, endodermis-specific *CASP1* promoter (*pCASP1*) (31) and acquired longitudinal median and surface sections of endodermal cells on 5-d-old seedlings.

*LAC1-mCherry* fusion protein expressed under the control of the *CASP1* promoter was observed in endodermal cells (Fig. 1B) where it localized to the median position of the endodermal cell walls as well as to the edge of the cortex-facing cell wall (Fig. 1D and SI Appendix, Fig. S3B).

*LAC3-mCherry* protein could also be localized using its endogenous promoter and localized in a manner very similar to *LAC1-mCherry* (Fig. 1B). *LAC5-mCherry* localized to the CS position in the cell wall and to the edges of cortex-facing cell wall of the endodermis (Fig. 1D and SI Appendix, Fig. S3B).

*LAC5-* and *LAC13-mCherry* also accumulated preferentially at CS. Accumulation in cortex-facing cell wall corner and in the case of *LAC13*, intracellular, mobile compartments might be due to overexpression by the strong *CASP1* promoter (Fig. 1B and D and SI Appendix, Fig. S3B).

Finally, we attempted to localize *LAC16-mCherry* by expressing it from the strong *ELTP* promoter, active in differentiated endodermis (32). However, we could only observe a fuzzy, cytoplasm-like signal. This would indicate that the *LAC16* fusion protein is not secreted. We propose that the very weakly expressed *LAC16* might be a nonfunctional pseudogene (SI Appendix, Fig. S2C).

To ascertain that laccases indeed localize precisely to incipient CS, we colocalized *LAC3-* and *LAC13-mCherry* with *CASP1-GFP*, which localizes to the plasma membrane subjacent to the CS, called the Casparian strip membrane domain (CSD). Both proteins showed near-perfect colocalization at the median position (Fig. 1E). CASPs colocalize with other cell wall proteins at the CS, such as PEROXIDASE 64 (PER64) and ENHANCED

SUBERIN 1 (ESB1), both involved in CS formation (2, 33). Thus, laccases and peroxidases localize to the same cell wall domain in the endodermis. This contrasts with a previous report, in which fluorescently tagged LAC4 and PER64 were localized to distinct cell wall domains in interfascicular fibers, with LAC4 localizing to the thick secondary cell wall, whereas PER64 localized to the cell wall corners and middle lamellae (15). In the endodermis, by contrast, where there is no apparent secondary cell wall, PER64 and LAC3 appear to reside in the same cell wall domain. Taken together, we found that LAC1, LAC3, LAC5, and LAC13 localize to the central median region of the endodermal cell wall, where the CS is formed.

**An *lac1 3 5 7 8 9 12 13 16* Nonuple Mutant Does Not Have Any Discernable Defect in CS Formation.** In order to test whether the LACs with enriched endodermal expression and CS localization are indeed required for lignin polymerization in the CS, we generated an *lac1 lac3 lac5 lac13 lac16* quintuple mutant (hereafter referred to as *5x lac*) by combining T-DNA insertion alleles for *LAC1*, *LAC5*, *LAC13*, and *LAC16* (*lac1*, *lac5*, *lac13*, *lac16*; hereafter referred to as *4x lac*) into which we generated an *lac3* mutant allele via CRISPR-Cas9 (34, 35), targeting the first exon of *LAC3* (SI Appendix, Fig. S4). Single *lac3* alleles were also generated and tested (SI Appendix, Figs. S4C and S5 A and C). To our surprise, we were unable to observe any difference in signal strength, structure, or position of the CS, as visualized by histological stains (SI Appendix, Fig. S6A).

Since the specific expression pattern, as well as their specific subcellular localization, strongly suggested an important function of laccases in CS formation, we decided that the most probable explanation for an absence of defects is a higher than suspected degree of redundancy among the laccases. We therefore selected an additional set of four *LACCASE* genes based on published, cell type-specific RNA profiling datasets, focused on the endodermis (27, 28). Moreover, we integrated recent RNA profiling data after SCHENGEN pathway stimulation in which *LACCASE 12* was found to be up-regulated, possibly compensating for a lack of activity in the *5x lac* mutant. Using a multiplexed guideRNA cloning strategy, we used six single guide RNAs (sgRNA) targeting four *LAC* genes. We used two guides for *LAC7*, two for *LAC8* (one targeting also *LAC9*), and two guides for *LAC12* (SI Appendix, Fig. S4B). With this multisgRNA construct, we were able to obtain mutant alleles of *LAC7*, *-8*, *-9*, and *-12* in the *5x lac* background, generating a *9x lac* mutant (SI Appendix, Figs. S4C and S5 A and C). Yet, despite having mutated the majority of *LACCASE* genes in the *Arabidopsis* genome—and all *LACCASES* with a significant, detectable expression in the endodermis—we were again unable to observe even a slight, quantitative difference in onset, strength, position, or function of CS in the endodermis (Fig. 2). Even when we challenged the endodermis with CIF2 peptide (a ligand of the SGN3 receptor that induces overlignification in cell corners) (6), we could not observe any delay or weaker accumulation of lignin (SI Appendix, Fig. S6 B and C), demonstrating that *LACCASES* are also not required for the less organized, cell corner lignification in the endodermis.

**A *per3 9 39 72 64* Quintuple Mutant Is Devoid of CSs.** Our inability to observe any indication for a role of laccases in CS lignification made it even more pressing to investigate whether peroxidases are indeed of critical importance for CS formation. As mentioned above, strong defects in lignification are observed only upon inhibitor treatments or pharmacological and genetic interference with ROS production, which implicates peroxidase activity only indirectly. Currently, direct genetic manipulation of peroxidases activities only led to partial, quantitative reductions in lignin content (20, 36, 37). This is almost certainly due to the sizeable number of secreted (type III) peroxidases, with 73 *PER*

members in *Arabidopsis thaliana* (38). Previously, our group had nevertheless attempted to genetically implicate peroxidases in CS lignification in the endodermis, focusing on *PER3* (AT1G05260), *PER9* (AT1G44970), *PER39* (AT4G11290), *PER64* (AT5G42180), and *PER72* (AT5G66390) as those that display the highest enrichment of expression in the endodermis (2). As for the laccases in this study, gene expression was confirmed by transcriptional reporters and demonstration that tagged peroxidases are secreted and accumulate at the CS in the endodermis (2) (SI Appendix, Figs. S7 and S10 A and C). The genetic analysis at the time revealed that a quadruple T-DNA insertion mutant of *per3*, *-9*, *-39*, and *-72* (hereafter referred to as *4x per*) did not have any discernable defect in the CS. With no T-DNA insertion lines available for the highly expressed *PER64* gene, a gene silencing approach was used. By generating an endodermis-specific, inducible amiRNA against *PER64* in the wild type, a significant delay in endodermal barrier formation could be observed (2). However, it could not be determined whether this partial defect resulted from specific *PER64* silencing or whether more *PER* genes were affected by endodermal amiRNA expression. Also, a direct visualization of CS lignification defects was not done at the time.

Using CRISPR-Cas9, we therefore generated a single *per64* mutant in wild-type plants, as well as a quintuple *per3 9 39 72 64* mutant (hereafter designated *5x per*) by transformation into the *4x per* mutant (SI Appendix, Figs. S5 B and D and S8). We found that the CS of *4x per* plants had no visible lignification defect, appearing identical to wild-type control (Fig. 3B). Interestingly, although the *per64* single mutant also displayed a seemingly normal CS, we observed an ectopic deposition of lignin in the edges of the cortex-facing cell wall of the endodermis. Yet, this signal was weak and mostly observed in the surface views (Fig. 3B). More strikingly, we found *5x per* mutant lines to be completely devoid of a CS (Fig. 3B). Interestingly, the endodermis retained its capacity to lignify, as we observed clear ectopic lignin depositions at the corner/edges of the pericycle- and cortex-facing cell walls (Fig. 3 A and B), with the intensity of fluorescent lignin at the cortex-facing cell wall being consistently more prominent than the one at the pericycle-facing one. This pattern of ectopic lignification is precisely reiterating the compensatory lignification observed in many other CS-defective mutants (31, 33, 39, 40). It is known to depend on SCHENGEN (SGN) pathway activation and eventually leads to an alternative, although significantly delayed, formation of an apoplastic diffusion barrier in CS mutants. We therefore assayed diffusion barrier formation in the *5x per* mutants. In wild-type plants, onset of propidium iodide (PI) uptake block occurred at around 14 cells (Fig. 3 C and D), and both single *per64* and the *4x per* mutant showed a similar onset of PI block. By contrast, *5x per* mutant lines displayed a strong delay in apoplastic barrier establishment (Fig. 3D), observed only after about 85 cells in both alleles (Fig. 3D). This delay is much stronger than in other mutants with defective CS and activated SGN pathway, such as *myb domain 36* (*myb36*), *esb1*, or *rbohF* (2, 33, 39) (SI Appendix, Fig. S8A). This is explained if the five mutated peroxidases were not only required for CS lignification but were also partially required for SGN-dependent compensatory lignification. This would then cause an additional delay in the establishment of the compensatory extracellular barrier through reduced cell corner lignification.

**A *PER64*-mCherry Fusion Construct Is Able to Complement the *5x per* Mutant Phenotype.** We then attempted to complement the phenotype of *5x per* mutants by introducing a C-terminal, fluorescently tagged *PER64* variant (*pPER64::PER64-mCherry-4G*) (SI Appendix, Fig. S10). For covisualization of lignin and *PER64*-mCherry-4G, lignin was stained with auramine-O in this case (41, 42) because its

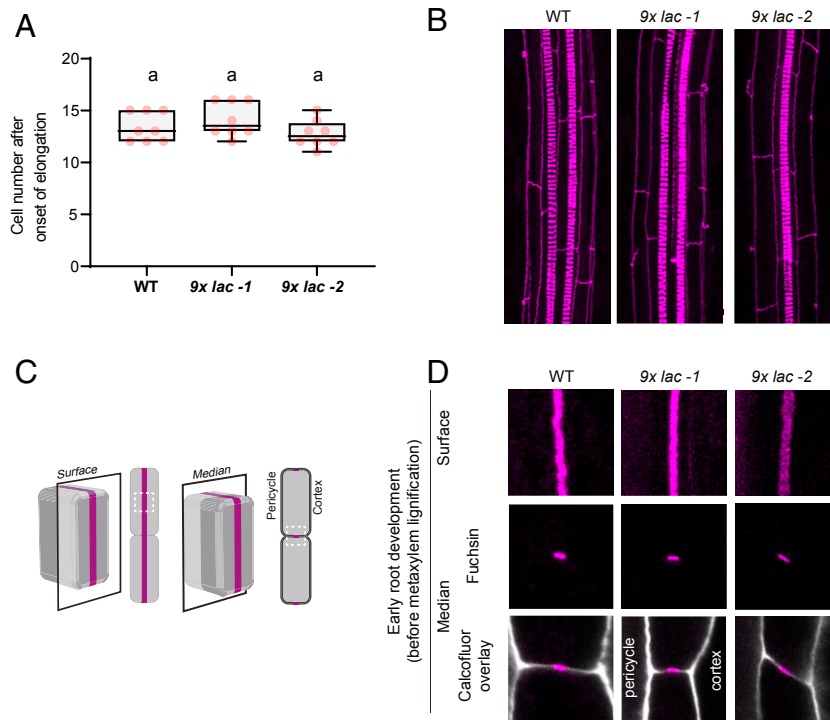


**Fig. 2.** Nonuple laccase mutants *lac1;3;5;7;8;9;12;13;16* (*9x lac*) deposit functional and lignified CS. (A) The CS in *9x lac* (nonuple) mutants still effectively seals the apoplast. Apoplastic barrier function of the endodermis is tested by the PI diffusion assay. Numbers indicate the endodermal cell in which apoplastic block is established, counting from the onset of endodermis cell elongation (mean,  $n = 8$  per genotype). One-way ANOVA and Tukey's test as post hoc analysis show no statistically significant difference. WT, wild-type Columbia (Col-0). (B) Basic fuchsin staining for visualization of lignin deposition in roots of two *9x lac* mutants compared with WT. Pictures show confocal z-axis maximum projections along the root, visualizing the CS networks and xylem vessels. Note the continuous, uninterrupted CS of the nonuple mutants. (C) Schematic of endodermal cell, explaining optical sections shown in D. Adapted from ref. 40. (D) Pictures of two *9x lac* mutants and WT displaying the surface and median views, as well as the overlay of cell wall and fluorescent lignin in the median view. Lines *9x lac-1* and *-2* carry different alleles (SI Appendix, Fig. S4). Lignin was stained with basic fuchsin in C and D, and cell wall was counterstained with calcofluor white M2R in D, following a modified version of the Clearsee protocol (41, 70). Representative picture at early root development taken at the 15th endodermal cell after onset of endodermal elongation. *9x lac*, *lac1;3;5;7;8;9;12;13;16*. (Scale bars: B, 20  $\mu\text{m}$ ; D, 5  $\mu\text{m}$ .)

green-spectrum emission does not overlap with mCherry. Two independent transformants displayed a CS indistinguishable from the wild type (SI Appendix, Figs. S10C and S11B), one of which with only some weak, ectopic lignification in some endodermal cells, similar in degree to what is observed in *per64* single mutant (SI Appendix, Fig. S11A). These slight remaining defects could be explained by either a lower activity of the PER64-mCherry fusion protein or slightly abnormal expression levels of PER64 by the promoter fragment used. Nevertheless, the complementation of the *5x per* mutant by the single PER64-mCherry remains impressive, with one line rescuing barrier formation to wild-type levels, while a second line also largely rescued, but with some delay of barrier formation compared with the wild type or the *4x per* mutant (SI Appendix, Fig. S11B). This also demonstrates that tagging with a fluorescent protein allows PERs involved in lignification to retain their functionality.

**5x per Plants Display Strongly Increased H<sub>2</sub>O<sub>2</sub> Accumulation in the Endodermis.** Peroxidases use H<sub>2</sub>O<sub>2</sub> as a cosubstrate during the oxidation of monolignols in the cell wall. We have previously demonstrated that ROS production observed in the endodermal cell wall is fully dependent on a pair of NADPH oxidases, RBOHD and F (2, 6). We therefore wondered whether an absence of the peroxidases utilizing ROS for lignin production would impact overall ROS levels. We resorted to the cerium chloride assay to detect hydrogen peroxide (43). H<sub>2</sub>O<sub>2</sub> reacts with cerium chloride to form cerium perhydroxide, producing electron-dense precipitates, readily detected in transmission

electron microscopy providing exquisite spatial resolution of ROS detection. This technique has been repeatedly used by our group to describe the pattern of H<sub>2</sub>O<sub>2</sub> localization in the endodermal cell wall (2, 6).

Roots of the wild type, *per64*, and *4x per* displayed peroxide precipitates that were largely restricted to the outer edge of the CS. Roots of *5x per* lines by contrast showed very prominent peroxide precipitates along an extended intercellular region between endodermal cells, while no indication of CS formation is observed in this region (Fig. 4B). This observation perfectly fits the expected consequences of impaired peroxidase activity in endodermal cell walls, which fails to consume the ROS produced by RBOHD and F by polymerizing CS lignin (6). It corroborates the model postulated for localized lignin deposition in the CS, in which local ROS production by NADPH oxidases is directly used by colocalizing cell wall peroxidases (2). Moreover, it suggests that peroxidase-mediated lignin polymerization represents a powerful ROS sink in vivo.

**Increased H<sub>2</sub>O<sub>2</sub> Accumulation and Remaining Lignification in the Endodermis of 5x per Plants Are Abrogated in SGN Pathway Mutants.** It was shown that activation of the SGN pathway depends upon the perception of two small signaling peptides, the Casparian strip Integrity Factors 1 and 2 (CIF1 and CIF2, respectively), by their receptor, the leucine-rich repeat receptor-like kinase SCHENGEN 3 (SGN3; also called GSO1), which in turn, activates a receptor-like cytoplasmic kinase, SCHENGEN 1 (SGN1) (4–6). While the CIF peptides are produced in inner

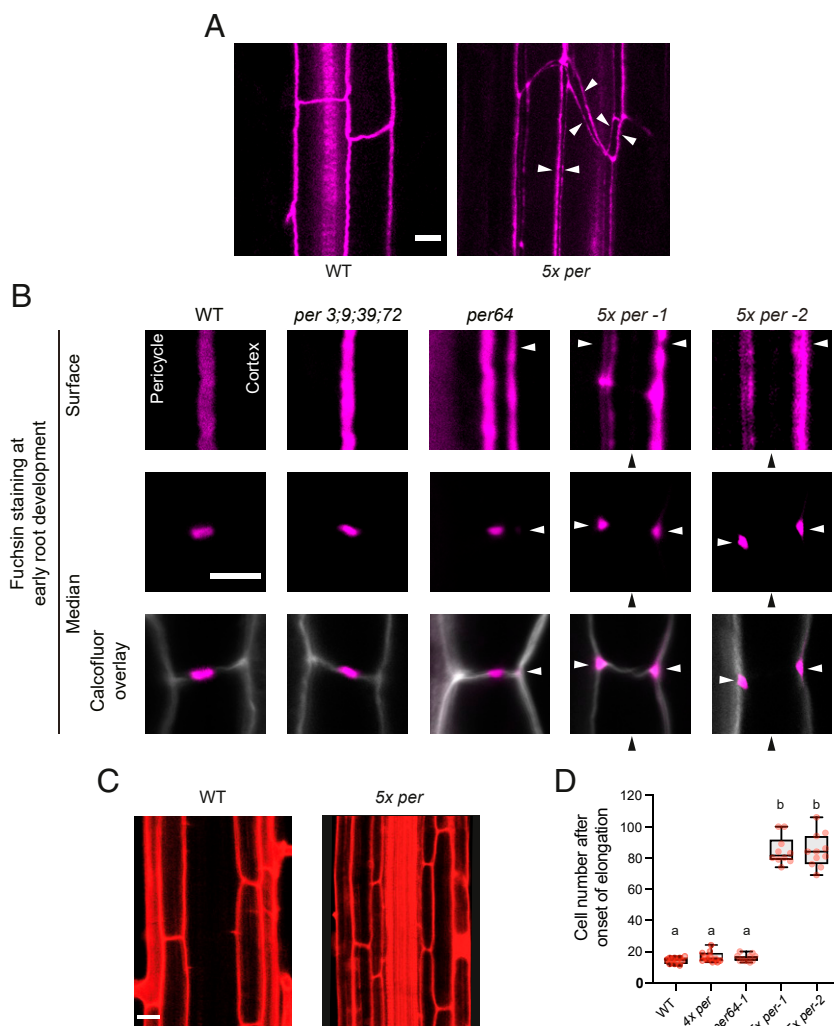


**Fig. 3.** Quintuple peroxidase mutants *per3;9;39;64;72* (*5x per*) are impaired in CS deposition. (A) Overview of lignin deposition in the endodermis of plants of wild-type Col-0 (WT) and the *5x per* mutants. White arrows point to ectopic basic fuchsin-positive deposits (lignin-like material). Note that this “double band” appearing in the *5x per* mutant is cell corner lignification, which is more easily observed in B. (B) Pattern of fluorescent lignin deposition in four peroxidase mutant genotypes compared with WT at early root development (before metaxylem lignification). Pictures displaying the surface and median confocal views, as well as the overlay of cell wall and fluorescent lignin in the median view. Black arrowheads point to the central cell wall position where the CS would normally form. White arrowheads point to ectopic deposits of lignin-like material. Lignin was stained with basic fuchsin, and cell wall was counterstained with calcofluor white M2R following a modified version of the Clearsee protocol (41, 70). *4x per*, *per3;9;39;72*. (C) The endodermis of *5x per* plants is permeable to the fluorescent apoplastic tracer PI (red), which enters to the stele, whereas in WT, it is blocked at the endodermis. Pictures were taken at 20 cells after onset of elongation of endodermal cells. (D) *5x per* plants have delayed establishment of apoplastic barrier. Apoplastic barrier function of the endodermis is tested by the PI diffusion assay. Numbers indicate the endodermal cell in which apoplastic block is established, counting from the onset of endodermis cell elongation (mean,  $n = 10$  seedlings per genotype; one-way ANOVA, and Tukey’s test as post hoc analysis; different letters indicate statistical significance;  $P < 0.005$ ). Lines *5x per-1* and *-2* carry different alleles (SI Appendix, Fig. S8E). (Scale bars: A, 10  $\mu\text{m}$ ; B, 5  $\mu\text{m}$ ; C, 20  $\mu\text{m}$ .)

cells of the vasculature, SGN1 is localized exclusively to the cortex-facing part of the plasma membrane, outside of the CSD (6, 44). This spatial disposition will lead to continuous activation of the pathway only when CS formation is defective and the diffusion barrier cannot be established. The CIF peptides thus effectively act as diffusion probes, initiating compensatory lignification whenever they succeed in reaching an SGN3–SGN1 signaling complex (6). Recently, it has been demonstrated that SGN3 drives lignification through a branched pathway (6). In one branch, SGN1 directly phosphorylates and activates NADPH oxidases at the plasma membrane, strongly activating ROS production. In the other branch, mitogen-activated protein (MAP) kinases are activated, and an induction of a large set of downstream genes is observed. Two peroxidases, PER15 and -49, are among the most highly up-regulated genes upon CIF stimulation

(6) (SI Appendix, Fig. S1E). The combination of enhanced ROS production and activation of peroxidase gene expression can directly account for the enhanced and ectopic lignification in cell corners in CS-defective mutants. In order to demonstrate that the ectopic lignification in the *5x per* mutant is also caused by SCHENGEN pathway activation, we generated a *cif1 cif2* double mutant in the *5x per* background, using a specific sgRNA to efficiently target both genes (SI Appendix, Fig. S12). Plants of *cif1 cif2* have a normally positioned but discontinuous CS without ectopic lignification (Fig. 5A). This incomplete CS closure in SGN pathway mutants is thought to reflect a partial requirement for this pathway in undisturbed, wild-type CS formation, possibly to provide a transient boost of CS formation, while the CS is in the process of being built and the diffusion barrier is still permeable. We found enhanced and ectopic accumulation of  $\text{H}_2\text{O}_2$

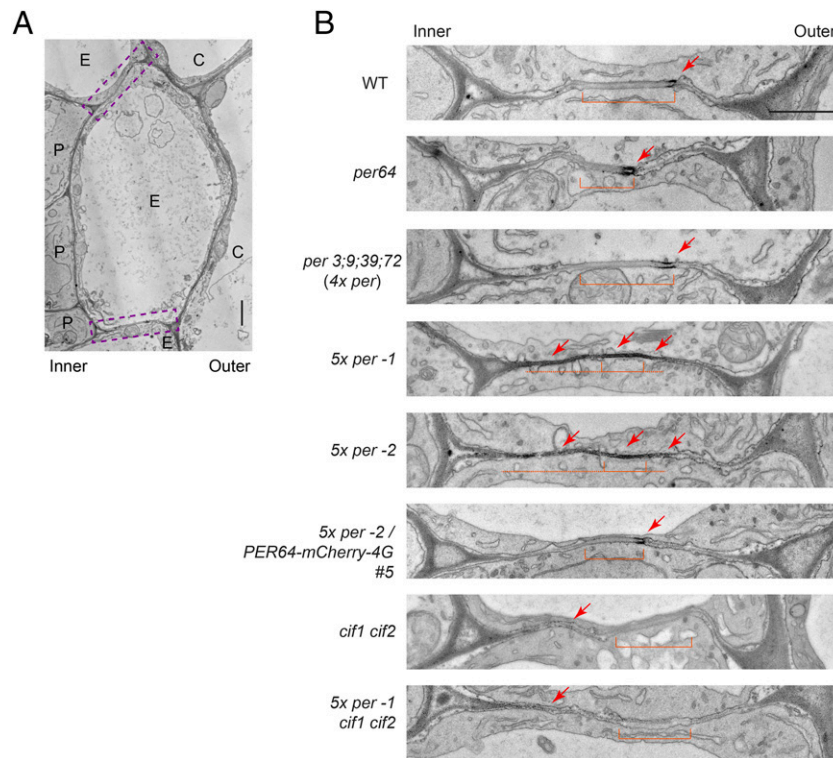


**Fig. 4.** Mutation of *PER3*, *-9*, *-39*, *-64*, and *-72* leads to enhanced and ectopic  $H_2O_2$  accumulation in the cell wall around the region where the CS normally forms. (A) Transmission electron micrograph of *A. thaliana* root in cross-section. Overview of the endodermal cell wall region displayed in B boxed in purple with a dotted line. "Inner" designates the pericycle-facing cell wall, while "Outer" indicates the cortex-facing one. C, cortex; E, endodermis; P, pericycle; WT, wild-type Col-0. (B) Micrographs show the median cell wall between endodermal cells. The cells shown correspond to the 1.3- to 1.5-mm region from the root tip of 5-d-old seedlings. Localized  $H_2O_2$  production is detected by the cerium chloride ( $CeCl_3$ ) assay.  $H_2O_2$  reacts with  $CeCl_3$  to form electron-dense precipitates of cerium perhydroxide. Arrows point to electron-dense precipitates. Brackets indicate CS (WT, *per64*, and *cif1 cif2*) or the region where the CS would normally localize (*5x per -1*, *5x per -2*, and *5x per -1 cif1 cif2*). Orange dotted line indicates extended region of ectopic  $H_2O_2$  precipitates. Note the absence of cerium perhydroxide precipitates in the median cell wall region in lines carrying the *cif1 cif2* mutations. Lines *5x per -1* and *-2* carry different alleles (*SI Appendix*, Fig. S8E). (Scale bars: A and B, 1  $\mu m$ .)

to be abrogated in the *5x per cif1 cif2* plants (Fig. 4B). Consistently, the *5x per cif1 cif2* mutant was devoid of ectopic lignin deposits in the endodermis at the root zone before metaxylem lignification (Fig. 5A). Ectopic lignification could be induced by external application of CIF2 peptide, illustrating that the observed absence of lignification is due to lack of SCHENGEN pathway activation (Fig. 5B). For reasons we do not understand, a weak but clearly detectable lignification still seems to form later during root development in the *5x per cif1 cif2* mutant (*SI Appendix*, Fig. S13A).

We also tested whether combining the *cif1 cif2* and *5x per* mutations would further enhance their defects in the establishment of an apoplastic barrier. In the PI diffusion assay, *cif1 cif2* and *5x per* mutants have similar delays (barrier closes at  $86 \pm 9$  cells and  $85 \pm 9$  cells, respectively) (*SI Appendix*, Fig. S9B). Nevertheless, *5x per cif1 cif2* plants have a stronger delay than both individual lines, blocking PI after  $117 \pm 8$  cells, essentially encompassing the entire root until the beginning of the hypocotyl (*SI Appendix*, Fig. S9B). This suggests that, while very inefficient, the SCHENGEN signaling pathway still contributes to the very late sealing of the apoplast at the endodermis in *5x per* plants. Interestingly, loss-of-function mutants plants of MYB36, a master regulator of a gene set essential for CS formation, and EXO70A1, a subunit of the exocyst complex required for protein positioning at the CS domain, despite not making any CS, seal the apoplast much earlier than *5x per* plants (39, 40) (comparative data shown for *myb36-2* in *SI Appendix*, Fig. S9A). Thus, it seems that mutation of *per3*, *-9*, *-39*, *-64*, and *-72* not only affects

the formation of CS but also lowers the plant's capacity to seal the apoplast in the absence of CS by compensatory lignification. This idea is supported by the fact that both *PER9* and *-72* (mutated in the *5x per* plants) are significantly induced upon SCHENGEN pathway stimulation (6) (*SI Appendix*, Fig. S1E).

**The CSD Forms in the Absence of Lignin and CS Peroxidases.** Finally, we checked whether inability to form CS in *5x per* plants was due to a disrupted CSD. We used CASP1-GFP as a marker since this transmembrane protein accumulates very strong and stable at the site of CS formation and is important for its formation. With the exception of *rbohF*, all mutants with a defective CS show a lack or mislocalization of CASP1-GFP (2, 40, 44–46). We found that CASP1-GFP localizes to the median region of the endodermal plasma membrane, as in the wild type (Fig. 6A and B). In addition, ESB1, a secreted protein that strictly colocalizes with CASP1-GFP and is necessary for its correct accumulation and localization, also localizes normally in the cell wall in *5x per* plants (Fig. 6C). LAC3 also continued to be localized to the CSD (Fig. 6D). Thus, peroxidases require the CSD for their localization, but the CSD can form independently of their presence and is also unaffected by the absence of lignin.

## Discussion

As discussed in the Introduction, we hold that the endodermis is an important model for studying lignification, complementing in interesting ways the study of xylem vessels and fibers that represent the vast majority of lignin produced in a mature plant.

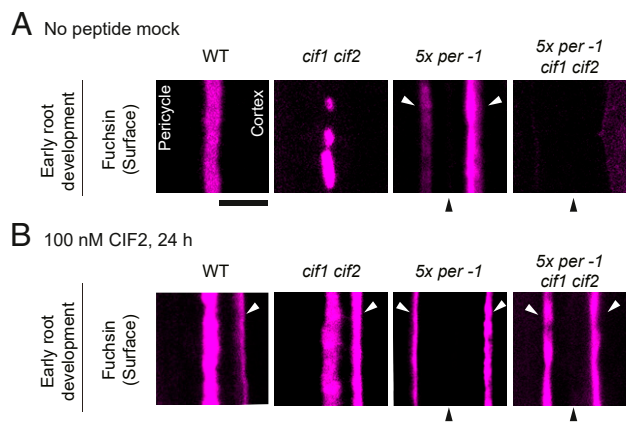


**Fig. 5.** Ectopic deposition of lignin-like material in *5x per* (*per3;9;39;64;72*) plants is dependent on the SCHENGEN pathway. (A) Surface confocal sections of the CS stained with basic fuchsin. Pictures were taken at early root development (before metaxylem lignification). WT, wild-type Col-0. (B) Same types of pictures were taken in roots of seedlings treated with 100 nM SGN3 receptor ligand CIF2 for 24 h. Black arrowheads indicate the wall position where the CS usually forms. White arrows point to ectopic basic fuchsin-positive deposits (lignin-like material). Fluorescent lignin was stained with basic fuchsin following a modified version of the Clearsee protocol (41, 70). (Scale bar: 5  $\mu$ m.)

Yet, in addition to this, lignification in the endodermis might also be more representative of a type of lignification that is widespread yet constitutes only a minor fraction of total lignin, occurring in cells with no, or little, secondary cell wall and in which lignin is deposited in a restricted fashion as part of a developmental program of differentiation (i.e., during peridermal differentiation or abscission zone formation) (17, 47) or as part of an induced stress response (i.e., during cell wall damage or bacterial invasion) (48, 49). Indeed, endodermal lignification occurs in the cell walls between two endodermal cells that amount to a total thickness of barely 200 nm (3, 31), very different in dimension from lignified secondary walls, which in the case of interfascicular fibers can be 10-fold thicker (ca. 2  $\mu$ m) (50, 51). Beyond this, primary and secondary walls also differ in composition and abundance of their cellulose, hemicellulose, and pectin components (52, 53). This raises the question of whether both types of cell walls require different ways of lignification, possibly mediated by different sets of enzymes. Indeed, it was reported that xylary fibers localize PER64 in a pattern resembling primary cell walls, while a laccase (LAC4) is localized exclusively to secondary cell wall domains (15), although a recent, more extensive study found localization of peroxidases and laccases to both primary and secondary cell walls in the same tissues (54). Taking advantage of a previous report showing that LAC4-mCherry fusion is functional in xylem cells (13), we used *pCASP1::LAC4-mCherry* constructs to test for complementation in *5x per* (SI Appendix, Fig. S14). Surprisingly, LAC4-mCherry is targeted to the median cell wall where the CS forms (SI Appendix, Fig. S14). Homozygous lines displayed an apoplastic block that is slightly less delayed, compared with *5x per*, indicating that overexpressed LAC4-mCherry can provide some degree of rescue. This observation suggests that there is some limited capacity of overexpressed laccases to compensate for lack of peroxidases when overexpressed, contributing to endodermal lignification and barrier formation. However, a detailed analysis of lignification in those lines would be required to draw further conclusions.

Previous studies using organ- and plant-wide analyses of *per* mutants only showed quantitative reduction in lignin content (19, 20, 55–57). Nevertheless, whether *PERs* are indeed essential for

lignification has remained unproven. With our focused approach on the CS, we now demonstrate that in *5x per* mutants, lignin polymerization in this specific structure is abolished, with a concomitant, local increase in ROS accumulation, illustrating a strong and direct requirement of *PERs*.

The *5x per* plants appear to be rather specifically impaired in CS formation, as they do not show obvious non-CS related phenotypes and can easily be propagated. This suggests that other lignin structures are unaffected or only weakly affected in this mutant and further supports the idea that subsets of *PERs* can play specific roles in various cellular contexts. *PER9* and *PER40*, for example, are required for anther and pollen development likely by enabling polymerization of extensin proteins in the cell wall, while *PER36* is required for seed coat mucilage extrusion and is proposed to regulate degradation of the outer cell wall (58, 59).

One speculation to account for the strong requirement of peroxidases, yet the lack of any phenotype in a *9x lac* mutant, would therefore be to postulate that laccases are expendable for lignification of primary cell walls but are required for lignification of secondary cell walls. While this is certainly consistent with and supported by the currently available data, it raises the question as to why a considerable number of nonrequired laccases would continue to be expressed in the endodermis and moreover, localize to CS. Monocotyledonous, and more rarely, dicotyledonous plants, form very thick secondary cell walls in the endodermis after suberization that can become lignified, but those occur very late in development (60). We are not aware that the much more short-lived endodermis of *Arabidopsis* would form any significant amounts of secondary walls that could become lignified. Recently, laccases were proposed to be important for CS formation (61), based on the effects of a copper chelator bathocuproinedisulfonic acid and the *N*-glycosylation inhibitor tunicamycin, both of which cause misorganization of lignin deposition in the CS, compromise the apoplastic barrier, and activate ectopic lignification. Based on the copper requirement for laccase activity, it was concluded that their activity is required for CS formation. However, no genetic evidence was provided, and it cannot be excluded that the effect of the two pharmaceutical treatments may be the result of disturbing the function of a much larger number of proteins. Indeed, Uclacyanins are both copper-containing and glycosylated proteins (62) and were recently shown to affect lignin deposition in the CS (63). Hence, these data can only be taken as an indication that copper-containing- and *N*-glycosylated-proteins, but not specifically laccases, are involved in CS localization.

There are several, not mutually exclusive, ways to explain the presence of laccases in the endodermis. 1) Laccases might be required for CS formation under specific conditions that are not encountered in our laboratory environment but sufficiently occur in nature to maintain their presence in CS. 2) A common transcription factor regulatory network might govern expression of lignification genes for many different cell types and condition. Such a transcriptional “lignification module” might be activated both in cells with secondary walls (requiring laccases) or in those with only primary wall (not requiring them). Supporting such an idea, an MYB transcription factor driving lignification was shown to be up-regulated in diverse cell types and conditions, such as pathogen attack, cell wall stress, or SGN pathway activation (5, 64, 65). In such a situation, the presence of “unnecessary” laccases might simply reflect the absence of a dedicated transcriptional module regulating expression of lignification genes in the endodermis. 3) Lack of obvious CS phenotypes in engineered *lac* mutants may result from RNA-based compensation mechanisms (66), which might support CS formation by up-regulation of homologous LACs. Recent studies showed that nonsense mutations created with CRISPR-Cas9 may lead to activation of homologous genes that compensate for the activity

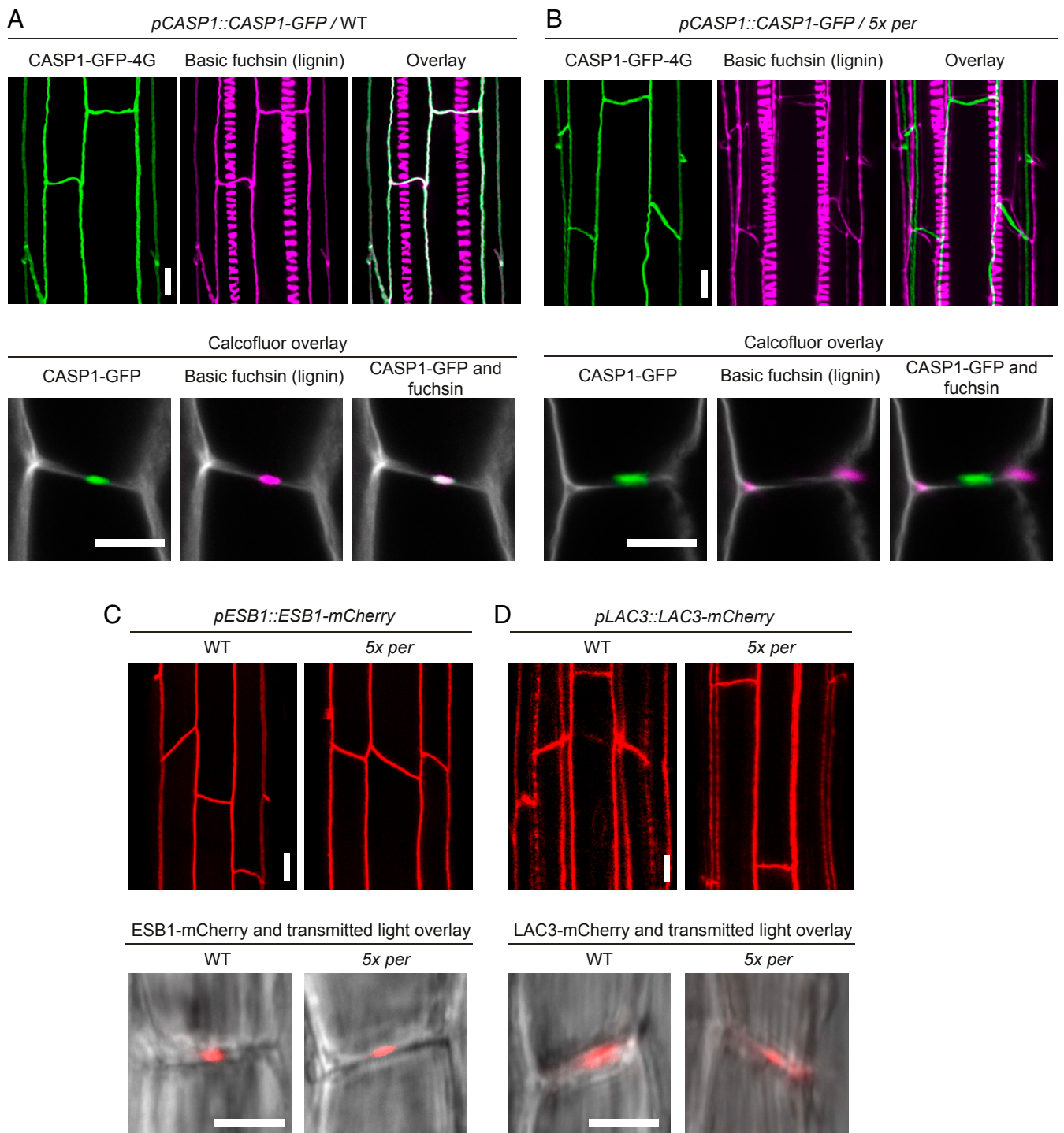


**Fig. 6.** Organization of proteins at the CS and CSD is unaltered in *5x per* plants. (A and B) CASP1-GFP-4G (green) labels the CSD in wild-type Col-0 (WT) plants (line #3-3-1) and colocalizes perfectly with CS lignin (magenta; colocalization: white). CASP1-GFP is targeted to the same domain in *5x per* plants (line #4-2-2) and does not colocalize with the cell corner lignin of the mutants. *Upper* shows three-dimensional (3D) reconstructions (z-axis maximum projections) of CASP1-GFP-4G and fuchsin (lignin staining). *Lower* shows pictures of median confocal views of the endodermis, displaying the overlay of CASP1-GFP-4G and fuchsin with calcofluor white M2R (cell wall staining, in gray). Samples were prepared with a modified version of the Clearsee protocol (41, 70). (C) ESB1-mCherry is targeted exclusively to the CS in the WT, which remains unaffected in *5x per* (line #6-1-1). *Upper* shows 3D reconstructions (z-axis maximum projections) of ESB1-mCherry. *Lower* shows median confocal views of the endodermis with ESB1-mCherry in overlay with transmitted light in gray. (D) LAC3-mCherry-4G localizes to the CS and the cortex-facing edges of the endodermal cell wall in the WT and is not altered in *5x per* (line #4-6). *Upper* shows 3D reconstructions (z-axis maximum projection) of LAC3-mCherry-4G. *Lower* shows median confocal sections of the endodermis with LAC3-mCherry-4G in overlay with transmitted light in gray. The 3D reconstruction for LAC3-mCherry in this panel is identical to that in Fig. 1 A and B. (Scale bars: A, *Upper*, B, *Upper*, C, *Upper*, and D, *Upper*, 10  $\mu$ m; A, *Lower*, B, *Lower*, C, *Lower*, and D, *Lower*, 5  $\mu$ m.)

of the mutated gene (66). To exclude this latter possibility, a careful monitoring of all of the remaining *LAC* genes for up-regulated expression in the endodermis will be necessary.

## Materials and Methods

**Plant Material and Growth Conditions.** For all experiments, *A. thaliana* (ecotype Columbia) was used. The following mutants were used in this study: *per3;9;39;72* (4x *per*; SALK\_140204, GABI\_186D03, SAIL\_369\_F11, and SAIL\_891\_H09, respectively) (2); *esb1-1* (67); *myb36-2* (*GK\_543B11*) (46); *rboh-f-3* (SALK\_059888) (2); *lac1* (SALK\_207114); *lac5* (SALK\_127394); *lac13* (SALK\_023935); *lac16* (SALK\_064093); *lac1;5;13;16* (4x *lac*) mutant was created by standard crossing procedures. A list of primers used for mutant genotyping is *SI Appendix, Table S1*. The following mutants were generated by CRISPR-Cas9 method (34, 35). For *per64*, a protospacer sequence compatible with the SpCas9 and StCas9 in ref. 35 was used in independent experiments. The SpCas9-compatible protospacer was deployed in the 4x *per* genetic background to create 5x *per* mutants. To obtain *lac3* alleles, we utilized a single protospacer sequence. LAC3 was mutated in the 4x *lac* genetic background to obtain the 5x *lac* mutants. In order to generate 9x *lac* mutants, a multiplex sgRNA cloning strategy was followed to target LAC7, -8, -9, and -12 in the 5x *lac* genetic background. Two sgRNAs were deployed simultaneously per each of these genes, except for LAC9, where only one sgRNA was used, which has a common target in LAC8. *cif1 cif2* mutants were generated using an sgRNA that targets both CIF1 and CIF2. A list with the sgRNA sequences is available in *SI Appendix, Table S2*. Protospacer sequences were designed with the CRISPR-P 2.0 design tool (<http://crispr.hzau.edu.cn/CRISPR2/>) (68) and Benchling (<https://www.benchling.com>). Transgenic plants with expression constructs were generated by transformation of *Arabidopsis* plants by the floral dip method (69). Seeds were surface sterilized by quick rinse in 70% EtOH, followed by 96% EtOH, dried and plated on half-strength Murashige and Skoog medium (MS) containing 0.8% agar plates, and vernalized at 4 °C for 2 to 3 d in the dark. Seedlings were grown vertically at 22 °C, under long-day conditions (18 h, 100 μE). All microscopic analyses were performed on roots of 5-d-old seedlings. For assays with CIF2 peptide, 4-d-old seedlings were transferred to half-strength MS plates supplemented with 1 μM, 100 nM, or water (untreated) for 1 d.

**Plasmid Construction.** Plasmids constructs were generated by Multisite gateway technology (Thermo Fisher Scientific). Promoter sequences were flanked by KpnI and XmaI sites, cloned into a p4-p1r donor vector, and then recombined by LR (attL- and attR-type recombination sequences) reaction to p221 NLS and p2r-p3 GFP-GUS to generate transcriptional reporters. The following promoters were used (base pairs [bp] before ATG): *pLAC1* (1,904 bp), *pLAC3* (2,111 bp), *pLAC5* (2,235 bp), *pLAC7* (2,021 bp), *pLAC13* (2,060 bp), and *pLAC16* (2,011 bp).

For translational fusion constructs, a destination vector of the type *pDem34GW,0* was used. The following expression plasmids were generated using the same promoter fragments cited above: *pLAC1::LAC1gDNA-mCherry-4G* (four glycine extension), *pLAC3::LAC3gDNA-mCherry-4G*, *pLAC5::LAC5gDNA-mCherry-4G*, *pLAC13::LAC13gDNA-mCherry-4G*, and *pLAC16::LAC16gDNA-mCherry-4G*. In addition, the following translational fusions were created using the *pCASP1* promoter: *pCASP1::LAC1gDNA-mCherry-4G*, *pCASP1::LAC3gDNA-mCherry-4G*, *pCASP1::LAC4gDNA-mCherry-4G*, *pCASP1::LAC5gDNA-mCherry-4G*, *pCASP1::LAC13gDNA-mCherry-4G*, and *pCASP1::LAC16gDNA-mCherry-4G*. The endodermis-specific *ELTP* promoter (32) was used to create the following construct: *pELTP::LAC16gDNA-mCherry-4G*. *pPER64::cgsPER64cgs-mCherry-4G* was generated using the respective entry clones of the *PER64* promoter and *CDS* sequence reported previously (2).

Cloning of plasmids used for CRISPR-Cas9 was performed as previously described. Briefly, the spacer to customize sgRNA for SpCas9 or StCas9 was cloned by annealing the oligos and then ligated into *BbsI*-linearized, Gateway-entry plasmid *pEn-Chimera* (34). For multiplex targeting of LAC7, -8, -9, and -12, the six sgRNAs utilized were cloned into two vectors, with either the fluorescence-accumulating seed technology (FAST) Red or FAST Green selection marker, each carrying three sgRNAs; 5x *lac* plants were cotransformed with both plasmids.

**Histological Techniques.** The PI diffusion assay was performed as previously described. Five-day-old seedlings were incubated in a solution of 15 μM PI for 10 min in the dark, then incubated in water for 30 s, mounted in water using a slide and coverslip, and immediately observed in microscope. Block of PI in the endodermis was quantified in terms of the number of endodermal cells

after onset of elongation. Onset of elongation was defined as the point where the length of an endodermal cell was more than twice its width. Col-0 was always included as control.

For visualization of CSs, cell wall, and fluorescent proteins, a modified protocol of ClearSee was used (41, 70). The CS was stained with the lignin dye basic fuchsin (0.2%. Fluka; Analytical; Chemical Abstracts Service (CAS)-No: 58969-01-0). Polysaccharide cell wall was stained with 0.1% calcofluor white M2R (Polysciences; catalog no. 4359).

**Confocal Laser Scanning Microscopy Imaging.** Confocal laser scanning microscopy experiments were performed on a Zeiss LSM 880 or a Leica SP8X microscope. All combinatorial fluorescence analyses were run as sequential scans. The following excitation and emission settings were used to obtain specific fluorescence signals: PI, 488/600 to 620 nm; Basic Fuchsin, 561/570 to 650 nm; Auramine-O, 488/505 to 530 nm; EGFP, 488/500 to 550 nm; mCherry, 561/600 to 650 nm; and Calcofluor white, 405/425 to 475 nm. Confocal images were processed and analyzed using the Fiji package of ImageJ (<https://fiji.sc>).

**Complementation of 5x per Mutant.** 5x *per* complementation was performed by transformation rescue. 5x *per-2* was transformed with *pPER64::cgsPER64-mCherry-4G* (where *cgs* stands for coding sequence), and 13 independent first generation of transformant (T1) lines were selected based on PER64-mCherry signal at the expected subcellular localization. Subsequently, presence of CS lignin in T2 individuals was tested by imaging 5-d-old seedlings stained with auramine-O, which was corroborated in all samples. However, only three lines (#5, #13, and #14) in which the PER64-mCherry lignification led to continuous CS, with none or seldom ectopic lignin deposits in individual endodermal cells, were selected for apoplastic barrier test, with PI in homozygous T3 5-d-old seedlings. Only lines #5 and #14 had rescue with apoplastic block values closest to wild-type Col-0. Segregant individuals lacking the PER64-mCherry transgene (FAST-Red negative) in those lines had no rescue compared with 5x *per*.

**Transmission Electron Microscopy for Detection of H<sub>2</sub>O<sub>2</sub> by the Cerium Chloride Assay.** Visualization of H<sub>2</sub>O<sub>2</sub> around the CS was done by the cerium chloride method as described in previous reports (2, 6, 43) with some modifications. The histochemical method is based on the generation of cerium perhydroxides as described and was used for the location of H<sub>2</sub>O<sub>2</sub> at the CS. Cerous ions (Ce<sup>3+</sup>) react with H<sub>2</sub>O<sub>2</sub> forming electron-dense cerium perhydroxide precipitates, which are detected by electron microscopy.

Five-day-old seedlings were incubated in 50 mM 3-[*N*-morpholino] propanoic sulphonic acid (Mops; pH 7.2) containing freshly prepared 10 mM cerium chloride (CeCl<sub>3</sub>) for 30 min. After the incubation with CeCl<sub>3</sub>, seedlings were washed twice in Mops buffer for 5 min and fixed in glutaraldehyde solution (EMS) 2.5% in 100 mM phosphate buffer (pH 7.4) for 1 h at room temperature. Then, they were postfixed in osmium tetroxide 1% (EMS) with 1.5% potassium ferrocyanide (Sigma) in phosphate buffer for 1 h at room temperature. Following that, the plants were rinsed twice in distilled water and dehydrated in ethanol solution (Sigma) at gradient concentrations (30%, 40 min; 50%, 40 min; 70%, 40 min; 100%, 1 h, twice). This was followed by infiltration in Spurr resin (EMS) at gradient concentrations (Spurr 33% in ethanol, 4 h; Spurr 66% in ethanol, 4 h; Spurr 100%, 8 h, twice) and finally polymerized for 48 h at 60 °C in an oven. Ultrathin sections 50-nm thick were cut transversally at 1.3 ± 0.1 mm from the root tip on a Leica Ultracut (Leica Mikrosysteme GmbH) and picked up on a nickel slot grid 2 × 1 mm (EMS) coated with a polystyrene film (Sigma). Micrographs were taken with a transmission electron microscope FEI CM100 (FEI) at an acceleration voltage of 80 kV, 11,000 magnifications (pixel size of 1.851 nm, panoramic of 17 × 17 pictures), and exposure time of 800 ms, with a TVIPS TemCamF416 digital camera (TVIPS GmbH) using the software EM-MENU 4.0 (TVIPS GmbH). All of the pictures were taken using the same beam intensity and panoramic aligned with the software IMOD (71).

**Data Availability.** All study data are included in the article and *SI Appendix*.

**ACKNOWLEDGMENTS.** We thank Edouard Pesquet and Edward E. Farmer for discussions on the project. We also thank the Central Imaging Facility and Electron Microscopy Facility of the University of Lausanne for expert technical support. This work was supported by funds from a European Molecular Biology Organization (EMBO) long-term postdoctoral fellowship (to Y.L. and R.U.), European Research Council (ERC) Consolidator Grant GA-N° 616228—ENDOFUN (to N.G.), Swiss National Science Foundation (SNSF) Grant CRSII3\_136278 (to N.G.), and SNSF Grant 31003A\_156261 (to N.G.), as

well as an overseas research fellowship from the Japan Society for the Promotion of Science (JSPS) (to S.F.). K.H. was supported by an AgreenSkills+ fellowship program, receiving funding from the European Union (EU)'s

Seventh Framework Programme Grant FP7-609398 and LabEx Saclay Plant Sciences (SPS) Grant Agence Nationale de la Recherche (ANR)-10-LABX-0040-SPS.

1. S. Naseer *et al.*, Casparian strip diffusion barrier in *Arabidopsis* is made of a lignin polymer without suberin. *Proc. Natl. Acad. Sci. U.S.A.* **109**, 10101–10106 (2012).
2. Y. Lee, M. C. Rubio, J. Allassimone, N. Geldner, A mechanism for localized lignin deposition in the endodermis. *Cell* **153**, 402–412 (2013).
3. N. Geldner, The endodermis. *Annu. Rev. Plant Biol.* **64**, 531–558 (2013).
4. T. Nakayama *et al.*, A peptide hormone required for Casparian strip diffusion barrier formation in *Arabidopsis* roots. *Science* **355**, 284–286 (2017).
5. V. G. Doblas *et al.*, Root diffusion barrier control by a vasculature-derived peptide binding to the SGN3 receptor. *Science* **284**, 280–284 (2017).
6. S. Fujita *et al.*, SCHENGEN receptor module drives localized ROS production and lignification in plant roots. *EMBO J.* **39**, e103894 (2020).
7. R. Vanholme, B. Demedts, K. Morreel, J. Ralph, W. Boerjan, Lignin biosynthesis and structure. *Plant Physiol.* **153**, 895–905 (2010).
8. J. Barros, H. Serk, I. Granlund, E. Pesquet, The cell biology of lignification in higher plants. *Ann. Bot. (Lond.)* **115**, 1053–1074 (2015).
9. L. Pourcel *et al.*, TRANSPARENT TESTA10 encodes a laccase-like enzyme involved in oxidative polymerization of flavonoids in *Arabidopsis* seed coat. *Plant Cell* **17**, 2966–2980 (2005).
10. M. Liang, E. Davis, D. Gardner, X. Cai, Y. Wu, Involvement of AtLAC15 in lignin synthesis in seeds and in root elongation of *Arabidopsis*. *Planta* **224**, 1185–1196 (2006).
11. D. M. Brown, L. A. H. Zeeff, J. Ellis, R. Goodacre, S. R. Turner, Identification of novel genes in *Arabidopsis* involved in secondary cell wall formation using expression profiling and reverse genetics. *Plant Cell* **17**, 2281–2295 (2005).
12. S. Berthet *et al.*, Disruption of LACCASE4 and 17 results in tissue-specific alterations to lignification of *Arabidopsis thaliana* stems. *Plant Cell* **23**, 1124–1137 (2011).
13. M. Schuetz *et al.*, Laccases direct lignification in the discrete secondary cell wall domains of protoxylem. *Plant Physiol.* **166**, 798–807 (2014).
14. N. Vukašinović *et al.*, Microtubule-dependent targeting of the exocyst complex is necessary for xylem development in *Arabidopsis*. *New Phytol.* **213**, 1052–1067 (2017).
15. E. Yi Chou *et al.*, Distribution, mobility, and anchoring of lignin-related oxidative enzymes in *Arabidopsis* secondary cell walls. *J. Exp. Bot.* **69**, 1849–1859 (2018).
16. Q. Zhao *et al.*, Laccase is necessary and nonredundant with peroxidase for lignin polymerization during vascular development in *Arabidopsis*. *Plant Cell* **25**, 3976–3987 (2013).
17. Y. Lee *et al.*, A lignin molecular brace controls precision processing of cell walls critical for surface integrity in *Arabidopsis*. *Cell* **173**, 1468–1480.e9 (2018).
18. H. Khandal, A. P. Singh, D. Chattopadhyay, The *MicroRNA397b-LACCASE2* module regulates root lignification under water and phosphate deficiency. *Plant Physiol.* **182**, 1387–1403 (2020).
19. J. Shigetō, Y. Kiyonaga, K. Fujita, R. Kondo, Y. Tsutsumi, Putative cationic cell-wall-bound peroxidase homologues in *Arabidopsis*, AtPrx2, AtPrx25, and AtPrx71, are involved in lignification. *J. Agric. Food Chem.* **61**, 3781–3788 (2013).
20. J. Shigetō *et al.*, Simultaneously disrupting AtPrx2, AtPrx25 and AtPrx71 alters lignin content and structure in *Arabidopsis* stem. *J. Integr. Plant Biol.* **57**, 349–356 (2015).
21. T. Laitinen *et al.*, A key role for apoplastic H<sub>2</sub>O<sub>2</sub> in Norway spruce phenolic metabolism. *Plant Physiol.* **174**, 1449–1475 (2017).
22. S. Koutaniemi *et al.*, Characterization of basic p-coumaril and coniferyl alcohol oxidizing peroxidases from a lignin-forming *Picea abies* suspension culture. *Plant Mol. Biol.* **58**, 141–157 (2005).
23. J. L. Pandey *et al.*, Investigating biochemical and developmental dependencies of lignification with a click-compatible monolignol analog in *Arabidopsis thaliana* stems. *Front. Plant Sci.* **7**, 1309 (2016).
24. S. M. Brady *et al.*, A high-resolution root spatiotemporal map reveals dominant expression patterns. *Science* **318**, 801–806 (2007).
25. A. Mustroph *et al.*, Profiling transcriptomes of discrete cell populations resolves altered cellular priorities during hypoxia in *Arabidopsis*. *Proc. Natl. Acad. Sci. U.S.A.* **106**, 18843–18848 (2009).
26. L. M. Liberman, E. E. Sparks, M. A. Moreno-Risueno, J. J. Petricka, P. N. Benfey, MYB36 regulates the transition from proliferation to differentiation in the *Arabidopsis* root. *Proc. Natl. Acad. Sci. U.S.A.* **112**, 12099–12104 (2015).
27. K. Vragović *et al.*, Transcriptome analyses capture of opposing tissue-specific brassinosteroid signals orchestrating root meristem differentiation. *Proc. Natl. Acad. Sci. U.S.A.* **112**, 923–928 (2015).
28. S. Li, M. Yamada, X. Han, U. Ohler, P. N. Benfey, High-resolution expression map of the *Arabidopsis* root reveals alternative splicing and lincRNA regulation. *Dev. Cell* **39**, 508–522 (2016).
29. P. V. Turlapati, K. W. Kim, L. B. Davin, N. G. Lewis, The laccase multigene family in *Arabidopsis thaliana*: Towards addressing the mystery of their gene function(s). *Planta* **233**, 439–470 (2011).
30. J. Allassimone, S. Naseer, N. Geldner, A developmental framework for endodermal differentiation and polarity. *Proc. Natl. Acad. Sci. U.S.A.* **107**, 5214–5219 (2010).
31. D. Roppolo *et al.*, A novel protein family mediates Casparian strip formation in the endodermis. *Nature* **473**, 380–383 (2011).
32. T. G. Andersen *et al.*, Diffusible repression of cytokinin signalling produces endodermal symmetry and passage cells. *Nature* **555**, 529–533 (2018).
33. P. S. Hosmani *et al.*, Dirigent domain-containing protein is part of the machinery required for formation of the lignin-based Casparian strip in the root. *Proc. Natl. Acad. Sci. U.S.A.* **110**, 14498–14503 (2013).
34. F. Fauser, S. Schiml, H. Puchta, Both CRISPR/Cas-based nucleases and nickases can be used efficiently for genome engineering in *Arabidopsis thaliana*. *Plant J.* **79**, 348–359 (2014).
35. J. Steinert, S. Schiml, F. Fauser, H. Puchta, Highly efficient heritable plant genome engineering using Cas9 orthologues from *Streptococcus thermophilus* and *Staphylococcus aureus*. *Plant J.* **84**, 1295–1305 (2015).
36. K. A. Blee *et al.*, A lignin-specific peroxidase in tobacco whose antisense suppression leads to vascular tissue modification. *Phytochemistry* **64**, 163–176 (2003).
37. N. Tokunaga, T. Kaneta, S. Sato, Y. Sato, Analysis of expression profiles of three peroxidase genes associated with lignification in *Arabidopsis thaliana*. *Physiol. Plant.* **136**, 237–249 (2009).
38. M. Tognolli, C. Penel, H. Greppin, P. Simon, Analysis and expression of the class III peroxidase large gene family in *Arabidopsis thaliana*. *Gene* **288**, 129–138 (2002).
39. T. Kamiya *et al.*, The MYB36 transcription factor orchestrates Casparian strip formation. *Proc. Natl. Acad. Sci. U.S.A.* **112**, 10533–10538 (2015).
40. L. Kalmbach *et al.*, Transient cell-specific EXO70A1 activity in the CASP domain and Casparian strip localization. *Nat. Plants* **3**, 17058 (2017).
41. R. Ursache, T. G. Andersen, P. Marhavý, N. Geldner, A protocol for combining fluorescent proteins with histological stains for diverse cell wall components. *Plant J.* **93**, 399–412 (2018).
42. E. Pesquet *et al.*, Novel markers of xylogenesis in zinnia are differentially regulated by auxin and cytokinin. *Plant Physiol.* **139**, 1821–1839 (2005).
43. C. S. Bestwick, I. R. Brown, M. H. R. Bennett, J. W. Mansfield, Localization of hydrogen peroxide accumulation during the hypersensitive reaction of lettuce cells to *Pseudomonas syringae* pv phaseolicola. *Plant Cell* **9**, 209–221 (1997).
44. J. Allassimone *et al.*, Polarly localized kinase SGN1 is required for Casparian strip integrity and positioning. *Nat. Plants* **2**, 16113 (2016).
45. A. Pfister *et al.*, A receptor-like kinase mutant with absent endodermal diffusion barrier displays selective nutrient homeostasis defects. *eLife* **3**, e03115 (2014).
46. B. Li *et al.*, Role of LOTR1 in nutrient transport through organization of spatial distribution of root endodermal barriers. *Curr. Biol.* **27**, 758–765 (2017).
47. A. Wunderling *et al.*, A molecular framework to study periderm formation in *Arabidopsis*. *New Phytol.* **219**, 216–229 (2018).
48. L. Denness *et al.*, Cell wall damage-induced lignin biosynthesis is regulated by a reactive oxygen species- and jasmonic acid-dependent process in *Arabidopsis*. *Plant Physiol.* **156**, 1364–1374 (2011).
49. M. H. Lee *et al.*, Lignin-based barrier restricts pathogens to the infection site and confers resistance in plants. *EMBO J.* **38**, e101948 (2019).
50. S. G. Hussey *et al.*, SND2, a NAC transcription factor gene, regulates genes involved in secondary cell wall development in *Arabidopsis* fibres and increases fibre cell area in *Eucalyptus*. *BMC Plant Biol.* **11**, 173 (2011).
51. S. Kushwah *et al.*, *Arabidopsis* XTH4 and XTH9 contribute to wood cell expansion and secondary wall formation. *Plant Physiol.* **182**, 1946–1965 (2020).
52. P. J. Harris, Primary and secondary plant cell walls: A comparative overview. *N. Z. J. For. Sci.* **36**, 36–53 (2006).
53. T. J. Simmons *et al.*, Folding of xylan onto cellulose fibrils in plant cell walls revealed by solid-state NMR. *Nat. Commun.* **7**, 13902 (2016).
54. N. Hoffmann, A. Benske, H. Betz, M. Schuetz, A. L. Samuels, Laccases and peroxidases co-localize in lignified secondary cell walls throughout stem development. *Plant Physiol.* **184**, 806–822 (2020).
55. F. Fernández-Pérez, F. Pomar, M. A. Pedreño, E. Novo-Uzal, Suppression of *Arabidopsis* peroxidase 72 alters cell wall and phenylpropanoid metabolism. *Plant Sci.* **239**, 192–199 (2015).
56. F. Fernández-Pérez, F. Pomar, M. A. Pedreño, E. Novo-Uzal, The suppression of AtPrx52 affects fibers but not xylem lignification in *Arabidopsis* by altering the proportion of syringyl units. *Physiol. Plant.* **154**, 395–406 (2015).
57. J. Herrero *et al.*, Bioinformatic and functional characterization of the basic peroxidase 72 from *Arabidopsis thaliana* involved in lignin biosynthesis. *Planta* **237**, 1599–1612 (2013).
58. J. R. Jacobowitz, W. C. Doyle, J. K. Weng, PRX9 and PRX40 are extensin peroxidases essential for maintaining tapetum and microspore cell wall integrity during *Arabidopsis* anther development. *Plant Cell* **31**, 848–861 (2019).
59. T. Kunieda *et al.*, Spatiotemporal secretion of PEROXIDASE36 is required for seed coat mucilage extrusion in *Arabidopsis*. *Plant Cell* **25**, 1355–1367 (2013).

60. D. E. Enstone, C. A. Peterson, F. Ma, Root endodermis and exodermis: Structure, function, and responses to the environment. *J. Plant Growth Regul.* **21**, 335–351 (2002).
61. Y. Zhuang, D. Zuo, Y. Tao, H. Cai, L. Li, Laccase3-based extracellular domain provides possible positional information for directing Casparian strip formation in *Arabidopsis*. *Proc. Natl. Acad. Sci. U.S.A.* **117**, 15400–15402 (2020).
62. A. M. Nersissian *et al.*, Uclacyanins, stellacyanins, and plantacyanins are distinct sub-families of phytocyanins: Plant-specific mononuclear blue copper proteins. *Protein Sci.* **7**, 1915–1929 (1998).
63. G. Reyt *et al.*, Uclacyanin proteins are required for lignified nanodomain formation within casparian strips. *Curr. Biol.* **30**, 1–9 (2020).
64. W. R. Chezem, A. Memon, F.-S. Li, J.-K. Weng, N. K. Clay, SG2-Type R2R3-MYB transcription factor MYB15 controls defense-induced lignification and basal immunity in *Arabidopsis*. *Plant Cell* **29**, 1907–1926 (2017).
65. T. Hamann, M. Bennett, J. Mansfield, C. Somerville, Identification of cell-wall stress as a hexose-dependent and osmosensitive regulator of plant responses. *Plant J.* **57**, 1015–1026 (2009).
66. M. A. El-Brolosy *et al.*, Genetic compensation triggered by mutant mRNA degradation. *Nature* **568**, 193–197 (2019).
67. I. Baxter *et al.*, Root suberin forms an extracellular barrier that affects water relations and mineral nutrition in *Arabidopsis*. *PLoS Genet.* **5**, e1000492 (2009).
68. Y. Lei *et al.*, CRISPR-P: A web tool for synthetic single-guide RNA design of CRISPR-system in plants. *Mol. Plant* **7**, 1494–1496 (2014).
69. S. J. Clough, A. F. Bent, Floral dip: A simplified method for agrobacterium-mediated transformation of *Arabidopsis thaliana*. *Plant J.* **16**, 735–743 (1998).
70. D. Kurihara, Y. Mizuta, Y. Sato, T. Higashiyama, ClearSee: A rapid optical clearing reagent for whole-plant fluorescence imaging. *Development* **142**, 4168–4179 (2015).
71. J. R. Kremer, D. N. Mastrorade, J. R. McIntosh, Computer visualization of three-dimensional image data using IMOD. *J. Struct. Biol.* **116**, 71–76 (1996).